

## ORIGINAL PAPER

**INDOOR MICROCLIMATIC VARIABLES ASSESSMENT BY VIBRATIONAL SPECTROSCOPY ON ORIGINAL STRUCTURE OF TROPAEUM TRAIANI MONUMENT, ADAMCLISI**

RADU LUCIAN OLTEANU<sup>1</sup>, CRISTIANA RADULESCU<sup>1,2\*</sup>, CLAUDIA STIHI<sup>2</sup>,  
IOANA DANIELA DULAMA<sup>1</sup>, CRISTINA MIHAELA NICOLESCU<sup>1</sup>,  
SORINA GEANINA STANESCU<sup>1</sup>, IOAN ALIN BUCURICA<sup>1</sup>,  
ION VALENTIN GURGU<sup>1</sup>, RALUCA MARIA STIRBESCU<sup>1</sup>,  
ANCA IRINA GHEBOIANU<sup>1</sup>, DORIN DACIAN LET<sup>1</sup>, SOFIA TEODORESCU<sup>1</sup>,  
LIVIU OLTEANU<sup>1</sup>, NICOLAE MIHAIL STIRBESCU<sup>1</sup>

---

*Manuscript received: 22.10.2020; Accepted paper: 12.11.2020;*

*Published online: 30.12.2020.*

**Abstract.** *This work attempts to show the usefulness of vibrational spectroscopy (i.e., FTIR and Raman) in the analysis of major components of the original structure materials of a heritage monument (Tropaeum Traiani, Adamclisi). The features of materials and indoor microclimatic variables (i.e., temperature and relative humidity), on the periods of the monitoring campaigns, were considered. As the conservation must make sure about the physicochemical and structural aspects of the materials, assessment of the environmental impact, deterioration processes and characterization of ancient building materials are useful to understand the chemical evolution in the past, predict the various trends in the future, choose the suitable restoration methods to preserve their present state, and even to describe the alteration process of materials and modification through time. The surface of original structure materials used until present seems not to be affected at major scale by the indoor microclimate variables. But even high recorded relative humidity levels promote the occurrence of amorphous calcium carbonate, calcite, aragonite and vaterite highlighted by vibrational spectroscopy data (i.e., FTIR and Raman), as a first effect, the development of biological organism can be enhanced, depending on the characteristics of the substrate. Second, atmospheric pollutants can be dissolved easier in the humidity existing in the porous material, and lastly, if the waterflow inside the stone is not homogeneous, cracks could appear due to differences in permeability.*

**Keywords:** *ancient monument; non-invasive analysis; FTIR; Raman spectroscopy; temperature; relative humidity; degradation.*

## 1. INTRODUCTION

Historical and cultural heritage assets are exposed to weather and submitted to influence of environmental parameters. Physicals, chemicals and biological factors interact with constitutive materials inducing changes both in its compositional and structural

---

<sup>1</sup> Valahia University of Targoviste, Institute of Multidisciplinary Research for Science and Technology, 130004 Targoviste, Romania.

<sup>2</sup> Valahia University of Targoviste, Faculty of Sciences and Arts, Department of Sciences and Advanced Technologies, 130004 Targoviste, Romania.

\*Corresponding Author: [radulescucristiana@yahoo.com](mailto:radulescucristiana@yahoo.com).

characteristics [1]. The decay of rocks and freshly exposed monumental stones is a complex process in which physical and chemical mechanisms are usually considered the main factors, it generally starts with alteration processes due to the synergetic action of rain, wind, sunlight and freezing/thawing cycles. Moreover, the atmospheric pollutants form deposits of particles, black encrustation and leave secondary reaction products on stone surfaces [2]. The consequence of these combined actions is a loss of cohesion with dwindling and scaling of stone material and with general weakening of the superficial structural strength [1-3].

An archeological complex of great significance, one of the most valuable ancient Roman monuments on the Romanian territory, was discovered at the beginning of the twentieth century; they are the ruins of the triumphal monument and of the fortress of Tropaeum Traiani, located in the present locality Adamclisi, Constanta County [4]. It is not known how long the triumphal monument has been unbroken. It seems that in the second and third centuries A.D., it suffered degradation caused by earthquakes or human activity. He was rebuilt in 1974-1977, after one of the hypothetical models of the old monument in ruins; parts of the original can be found in the museum housed inside it. The monument was rebuilt with a new technology using a metal structure clad with stone pieces from the same quarry exploited 2000 years ago [5]. All these stages of monument reconstruction are fully presented in papers published after 1960 [6-10].

The weathering of stone particularly, due to the outdoor/indoor climatic conditions and to particulate matters, has been studied by qualitative infrared analysis. On the other hand, the reflection measurements were used to investigate the effects of temperature, relative humidity (RH), and pollutants on marble. [2, 11-15]. Salt deposits, accretions and weathered surfaces on stone sculptures and buildings were investigated by IR spectroscopy according to different studies [16-19]. Calcium oxalate has been investigated as a weathering product formed by the action of lichens on stone [20]. Other authors have quantitatively measured calcium oxalate [21] or examined the stability of calcium oxalate hydration states [22] while determining its potential for protecting underlying stone [23].

Fourier transform infrared spectroscopy (FTIR) is commonly applied to the characterization of cultural heritage materials. More specifically, the FTIR non-invasive technique was often used in architectural heritage conservation due to the minimal amount of sample required and the rapid results of the analysis [24-26]. FTIR spectroscopy is required not only to exactly characterize the nature of the compounds (e.g., organic/inorganic) from original materials, but also to obtain precise chemical and physical information about ongoing changes. Hence, these significant aspects for cultural heritage conservation are essential to diagnose and to make the decisions on different processes of reconstruction/ rehabilitation/ preservation. [27]. Nowadays new opportunities are offered by ATR imaging spectroscopy as well. In ancient Rome, "Roman mortar" known as hydraulic materials such as ground volcanic ash, ceramic debris, and grinding bricks had been widely used in building materials [23, 28, 29]. FTIR technique as the molecular analysis is presented in an integrated approach with other analytical techniques including Raman spectroscopy.

Raman spectroscopy has proved to be a reliable technique that not only identifies carbonates of calcite structure [30], but also the calcium carbonate polymorphs [31, 32], as it can provide specific fingerprint spectra. There have been attempts to quantify mixtures containing the three anhydrous polymorphs (calcite, aragonite and vaterite) with successful application of Raman spectroscopy and X-Ray diffraction on mixture of the calcium carbonate polymorphs [32, 33]. Moreover, Raman technique allows the detection of hydrated amorphous and crystalline phases which are considered as precursors for the anhydrous calcium carbonate polymorphs [30]. The use of Raman analysis provides molecular characterization, which can aid in the inference of reactions taking place in the studied medium; in the context of construction materials, this technique can identify both main

components and trace elements of building stones and cementitious materials in addition to common nitrates and sulphates and some of their degradation products [34]. On the other hand, Raman spectroscopy is a non-invasive technique useful for the characterization of architectural heritage due to its reliable, fast, sensitive, and non-destructive features. Moreover, both FTIR and Raman spectroscopies, through their different mechanisms and selection rules, measure different vibrational modes and therefore provide complementary information on the analyzed materials [24].

As the conservation must make sure about the physicochemical and structural aspects of the materials, assessment of the environmental impact, deterioration processes and characterization of ancient building materials are beneficial for scientists or engineers to understand the chemical evolution in the past, predict the various trends in the future, choose the suitable restoration methods to preserve their present state, and even to describe the alteration process of materials and modification through time.

This work attempts to show the usefulness of vibrational spectroscopy (i.e., FTIR and Raman) in the analysis of major components of the original structure materials of Tropaeum Traiani, triumphal monument, Adamclisi, Romania. The features of materials and indoor microclimatic variables (i.e., temperature and relative humidity), on the periods of the monitoring campaigns, were considered. Spectral results in terms of spatial resolution, data quality, and chemical information obtained are presented in correlation with microclimatic data obtained in monitoring campaigns conducted in the period of August 2018 to August 2020. In future studies, the spectral data will be correlated with further elemental analyses (e.g., XRD, XRF, and ICP-MS) to characterize and estimate the stability of original structure materials under indoor/outdoor climatic conditions in a well-established period.

## 2. MATERIALS AND METHODS

### 2.1. SAMPLING

The monument was imaginary divided into four sections in height so that the collected samples to be spatial evenly distributed; at same points (Fig. 1) the microclimatic parameters were also monitored by means of portable devices).

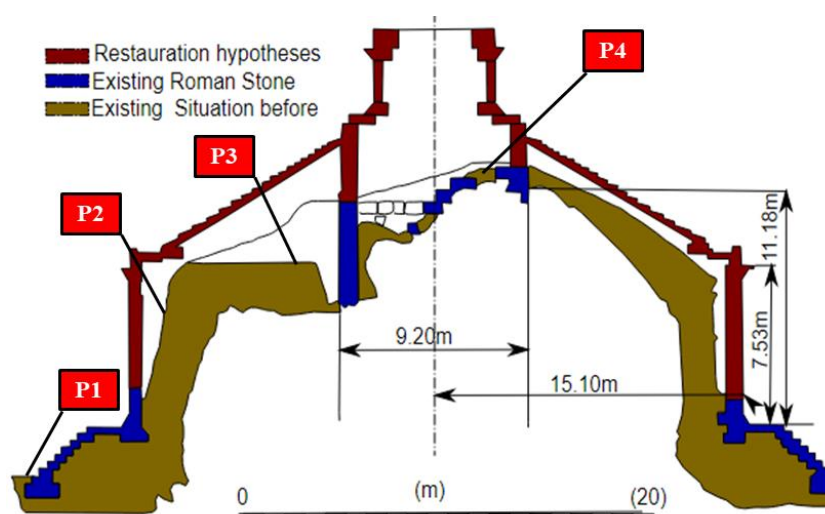


Figure 1. Tropaeum Traiani (Adamclisi) SV-NE cross-section from restored monument [39]; location of the sampling and measurement (microclimatic monitoring) points (P1 – P4).

The samples were collected on the same day and under same conditions (using disposable gloves, plastic utensils and packaged in plastic bags for further analysis) from the surface of the original structure. At the level of the four points, both rock and binder / mortar samples were collected.

It is known that Romans successfully improved on masonry structures the use of hydraulic lime mortars produced by combining lime with pozzolans [35-37]; hydraulic lime mortars are made by mixing lime with pozzolans (finely powdered materials which can be added to lime mortar to increase durability and to provide a positive set' [38]) or by developing hydraulic phases through the calcination of silica rich limestone directly quarried or synthetically mixed [35].

## 2.2. MICROCLIMATIC VARIABLES RECORDING

The positioning of the microclimate parameters recording devices aimed to measure the temperature and relative humidity (RH) in same points (Fig. 1) where sampling was achieved. The data acquisition was made during August 2018 and August 2020, obtaining a total of approximately 4200 records. Minimum and maximum values of the two variables measured by mobile device and Weather Station are shown in Tables 5-6 and Figs. 6-10.

The Weather Station PCE-FWS 20 (PCE Instruments UK Ltd) allow to detect with accuracy wind direction and speed, temperature, relative humidity and rainfall; the main characteristics, related with the two variables involved in the study were: indoor temperature range of 0÷50°C (0.1°C resolution), relative humidity measuring range of 10÷90% (1% resolution). Data acquisition was achieved with a recording frequency of 10 minutes continuously during monitoring period.

The mobile device used was a precision hygro-thermo-barometer GFB 200 (GSG Geologie-Service GmbH, Germany) equipped with Pt1000 temperature and capacitive polymer humidity sensor: temperature range of -25÷70°C (0.1°C resolution), relative humidity range of 0.0÷100.0% (1% resolution). Data acquisition was achieved with a recording frequency of 40 minutes during daytime.

## 2.3. FTIR AND RAMAN SPECTROSCOPY

The qualitative composition of stone and binder samples taken was characterized by vibrational spectroscopy, attenuated total reflectance-Fourier transform infrared spectroscopy (ATR-FTIR) and Raman spectroscopy. Spectral investigation of the compounds presents in the samples was performed by ATR-FTIR using a Vertex 80v spectrometer (Bruker, Germany), equipped with diamond ATR crystal accessory, for high refractive index bulk sample. The diamond ATR had a sampling area of approximately 0.5 mm<sup>2</sup>, and the infrared spectra were collected at 4 cm<sup>-1</sup> resolution over 22 scans. The important absorption frequencies were noted in the range of 1600–400 cm<sup>-1</sup>, as well as the fingerprint region of the spectra, with a resolution of 0.2 cm<sup>-1</sup> and 0.1% accuracy (transmittance). Raman spectral data were recorded with a portable Raman spectrophotometer Xantus-2-Rigaku ( $\lambda = 1064$  nm). The samples were analyzed in triplicate, without previous treatment, being used the average spectra.

### 3. RESULTS AND DISCUSSION

#### 3.1. INFRARED SPECTRAL ASSAY

FTIR and Raman data for stone slab samples have shown similarities concerning spectra in the wavenumber range of 4000-400  $\text{cm}^{-1}$  and 2000-200  $\text{cm}^{-1}$  respectively, with main spectral features in 1600-400  $\text{cm}^{-1}$  range (Tables 1-4, Figures 2-5); the observed peaks were assigned to different bonds according with their chemical structures.

**Table 1. Tentative assignments of significant peaks from FTIR and Raman spectra of construction materials based on type and year of sampling – point P1.**

Sample type	Sample code	Year	Wavenumber [ $\text{cm}^{-1}$ ] and relative intensity <sup>a</sup>	
<b>FTIR data</b>				
Stone slab	P1-a-18	2018	1796/1408/1086/873/800/712/464/443/420/400	w/s/m/s/w/s/w/w/w/w
	P1-a-20	2020	1796/1394/1085/872/712	w/s/w/s/m
Stone binder	P1-b-18	2018	1639/1415/1054/873/795/780/712/695/517/445/436	w/m/m/s/w/w/w/w/w/s/s
	P1-b-20	2020	1414/1068/874/795/712/455/418	s/s/s/w/m/w/w
<b>Raman data</b>				
Stone slab	P1-a-18	2018	1745/1426/1084/711/273	w/w/s/w/m
	P1-a-20	2020	1737/1421/1085/709/276	w/w/s/w/m
Stone binder	P1-b-18	2018	1947/1418/1304/1204/1084/953/825/693/273	s/w/w/w/m/w/w/w/w
	P1-b-20	2020	1850/1436/1292/1126/1085/770/710/490/451/230	w/m/m/w/m/s/s/m/m/m

<sup>a</sup>(s) strong; (m) medium; (w) weak.

**Table 2. Tentative assignments of significant peaks from FTIR and Raman spectra of construction materials based on type and year of sampling – point P2.**

Sample type	Sample code	Year	Wavenumber [ $\text{cm}^{-1}$ ] and relative intensity <sup>a</sup>	
<b>FTIR data</b>				
Stone slab	P2-a-18	2018	1793/1395/872/712/509/459/420/363	w/s/s/m/w/w/w/s
	P2-a-20	2020	1395/1087/872/712/379/361	s/w/s/s/w/s
Stone binder	P2-b-18	2018	3526/3400/1796/1682/1619/1421/1111/1040/873/796/781/712/672/600/457/393/380/361	m/m/w/w/m/s/s/s/w/w/w/s/w/s/m/m/s/s
	P2-b-20	2020	1415/1060/874/795/712/450/376/360	s/s/s/w/m/w/m/s
<b>Raman data</b>				
Stone slab	P2-a-18	2018	1738/1426/1084/711/273	w/w/s/w/m
	P2-a-20	2020	1737/1421/1085/709/276	w/w/s/w/m
Stone binder	P2-b-18	2018	1857/1745/1320/1227/1084/961/944/764/711/584/423/273	s/w/w/w/s/m/m/m/m/w/w/m
	P2-b-20	2020	1853/1744/1518/1421/1315/1222/1130/1085/970/780/710/510/441/256	s/w/w/w/w/w/w/s/m/s/s/w/w/s

<sup>a</sup>(s) strong; (m) medium; (w) weak.

Typical spectra of calcite-group carbonates include some major absorption bands between 4000-660  $\text{cm}^{-1}$  each of which may be identified with a particular deformational mode of the carbonate ion. These bands have been related to an out-of-plane bending, an asymmetric stretching and a planar bending of the carbonate radical [40, 41]. In the spectral range 1400-1480  $\text{cm}^{-1}$ , the broad vibrational band can be related to the presence of carbonate

ion (symmetric stretching mode of carbonate ion); also the present peaks in this spectral range can be related to amorphous calcium carbonate [35, 42].

The peaks from 1421/1428  $\text{cm}^{-1}$  (asymmetric stretching of carbonate radical), intense peak around 873  $\text{cm}^{-1}$  (out-of-plane bending of carbonate radical) and 712  $\text{cm}^{-1}$  (planar bending of carbonate radical) suggests the presence of both calcite and aragonite [35, 43]. The differences may be partially assigned to modifications involving lattice structure (a change in the coordination of the metal ion from six-fold in calcite to nine-fold in aragonite) and also to a change in lattice symmetry [40].

**Table 3. Tentative assignments of significant peaks from FTIR and Raman spectra of construction materials based on type and year of sampling – point P3.**

Sample type	Sample code	Year	Wavenumber [ $\text{cm}^{-1}$ ] and relative intensity <sup>a</sup>
<b>FTIR data</b>			
Stone slab	P3-a-18	2018	1796/1396/873/712/462/416/390/371
	P3-a-20	2020	1796/1394/872/712/417/376/361
Stone binder	P3-b-18	2018	1796/1413/1038/873/796/778/712/695/460/447/385/368
	P3-b-20	2020	1415/1064/874/799/712/452/430/397/369/358
<b>Raman data</b>			
Stone slab	P3-a-18	2018	1760/1426/1084/711/283
	P3-a-20	2020	1737/1421/1085/709/276
Stone binder	P3-b-18	2018	1920/1738/1588/1426/1312/1212/1084/945/782/711/602/253
	P3-b-20	2020	1870/1744/1418/1310/1222/1126/1085/970/780/710/582/460/256

<sup>a</sup>(s) strong; (m) medium; (w) weak.

**Table 4. Tentative assignments of significant peaks from FTIR and Raman spectra of construction materials based on type and year of sampling – point P4.**

Sample type	Sample code	Year	Wavenumber [ $\text{cm}^{-1}$ ] and relative intensity <sup>a</sup>
<b>FTIR data</b>			
Stone slab	P4-a-18	2018	2510/1796/1393/872/712/469/439/412/379/357
	P4-a-20	2020	1796/1396/1074/872/712/449/430/393/371/361
Stone binder	P4-b-18	2018	1795/1415/1062/873/797/780/712/694/452/378/362
	P4-b-20	2020	1796/1414/1061/969/873/796/780/712/446/359
<b>Raman data</b>			
Stone slab	P4-a-18	2018	1084/711/284
	P4-a-20	2020	1737/1421/1085/709/276
Stone binder	P4-b-18	2018	1920/1745/1426/1312/1204/1084/936/773/711/416/273
	P4-b-20	2020	1870/1744/1428/1310/1222/1126/1085/955/780/710/600/441/266

<sup>a</sup>(s) strong; (m) medium; (w) weak.

The transition is revealed by the appearance of an additional band (1393/1395  $\text{cm}^{-1}$ , a symmetric stretching mode characteristic of the carbonate ion but who does not ordinarily give rise to absorption in spectra of calcite group minerals) and splitting of the planar bending mode as well as by a shift in the wavenumber position of absorption bands common to both minerals. However, spectral variations within each group cannot be explained on this basis since the intra-group coordination remains constant. There are at least six different phases of

calcium carbonate: three anhydrous crystalline polymorphs (calcite, aragonite and vaterite) and three hydrated forms (crystalline monohydrate-monohydrocalcite, crystalline hexahydrate-ikaite, and an amorphous calcium carbonate hydrate) [30, 44, 45]. The physical properties of the material depend largely on the amount of each polymorph present [45].

The signals around  $1395\text{ cm}^{-1}$  suggest the formation of various coordinated bicarbonate groups which overlap calcium carbonate absorption bands [42, 46]. The presence of vaterite and calcite can be related with the peaks revealed around  $1085\text{ cm}^{-1}$  (medium/weak signals in FTIR spectra and strong signals in Raman spectra) and  $712\text{ cm}^{-1}$  respectively (medium/strong signals in FTIR and weak signals in Raman spectra) [33, 42, 47, 48]. Intense signals around  $1085\text{ cm}^{-1}$  in Raman spectra also suggest an overlapping of spectral bands due to the vaterite ( $1089\text{ cm}^{-1}$ ), calcite and aragonite ( $1084\text{ cm}^{-1}$ ) [33, 41]; also, other studies [30] point out that a broad signal with a sharp peak with a maximum at  $1083\text{ cm}^{-1}$  indicates the formation of crystalline calcium carbonates and amorphous calcium carbonate. Medium intensity band from  $1074\text{ cm}^{-1}$  (symmetric stretching mode of carbonate ion) can be due to the presence of strontianite (aragonite group) [40, 47].

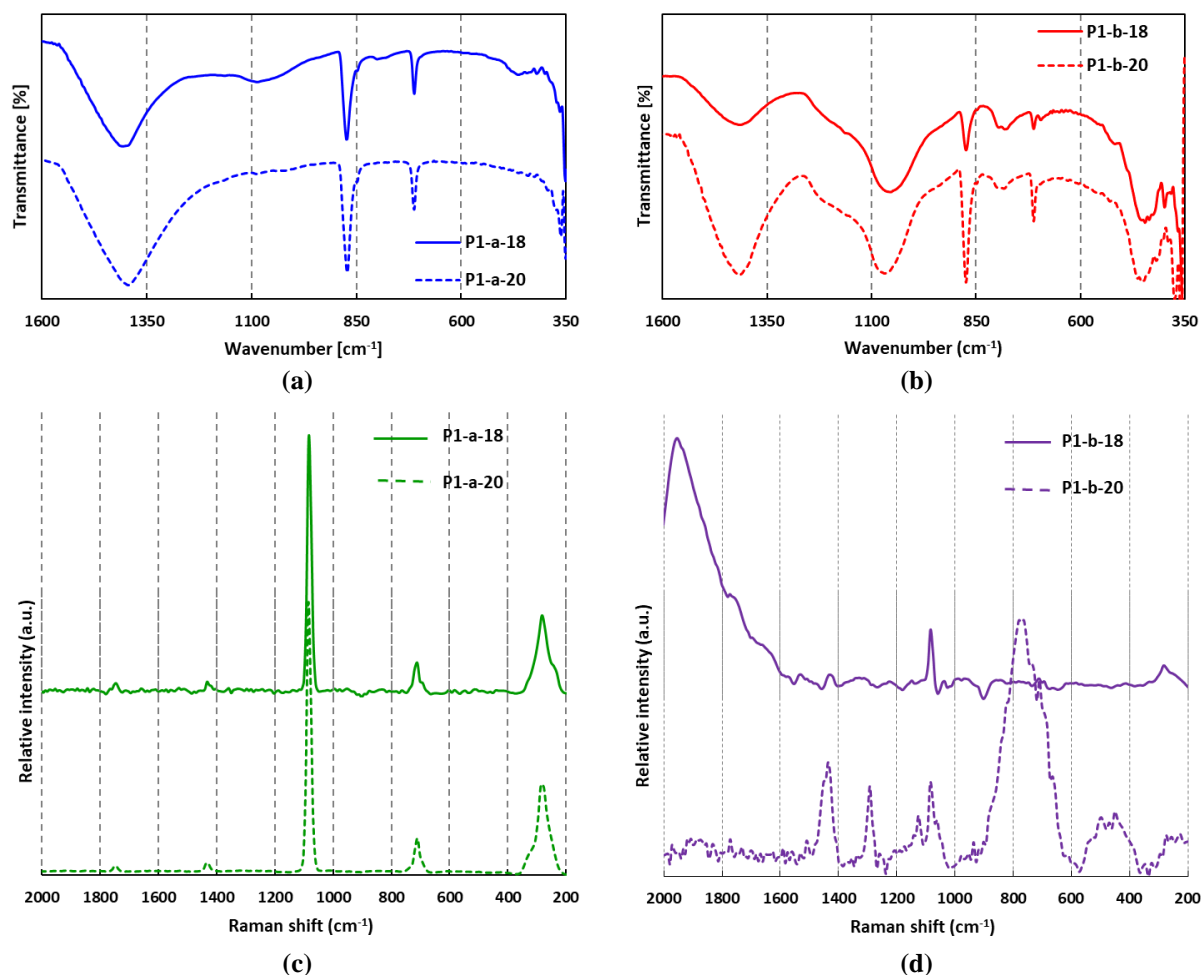


**Figure 2.** Overlaps of Fourier transform infrared (FTIR) and Raman spectra for construction materials based on type and year of sampling – point P1: (a), (b) – FTIR spectra; (c), (d) – Raman spectra.

Amorphous calcium carbonate absorption bands can be assigned in the  $1500\text{--}1400\text{ cm}^{-1}$ ,  $1100\text{--}1000\text{ cm}^{-1}$ ,  $900\text{--}800\text{ cm}^{-1}$  and close to  $700\text{ cm}^{-1}$  spectral region [35, 41, 48]. The weak bands around  $1796\text{ cm}^{-1}$  and  $1745\text{ cm}^{-1}$  can be due to the combination of symmetric C-O stretching and O-C-O bending vibrational modes [48]. In the FTIR spectra of some of the stone slab samples (e.g. P1 and P2) also shows a medium/weak intensity band at  $1085\text{ cm}^{-1}$

coincident with the Raman active symmetric C-O stretching mode of the  $\text{CO}_3^{2-}$  anion in calcite [48]. The infrared and Raman active vibrations mode of the carbonate ion are also present at 1408 (asymmetric C-O stretching mode), 872 ( $\text{CO}_3$  out-of-plane deformation mode) and  $712 \text{ cm}^{-1}$  (OCO bending, in-plane deformation mode); calcite combination bands are also assigned by low intensity bands around  $1795 \text{ cm}^{-1}$  [48].

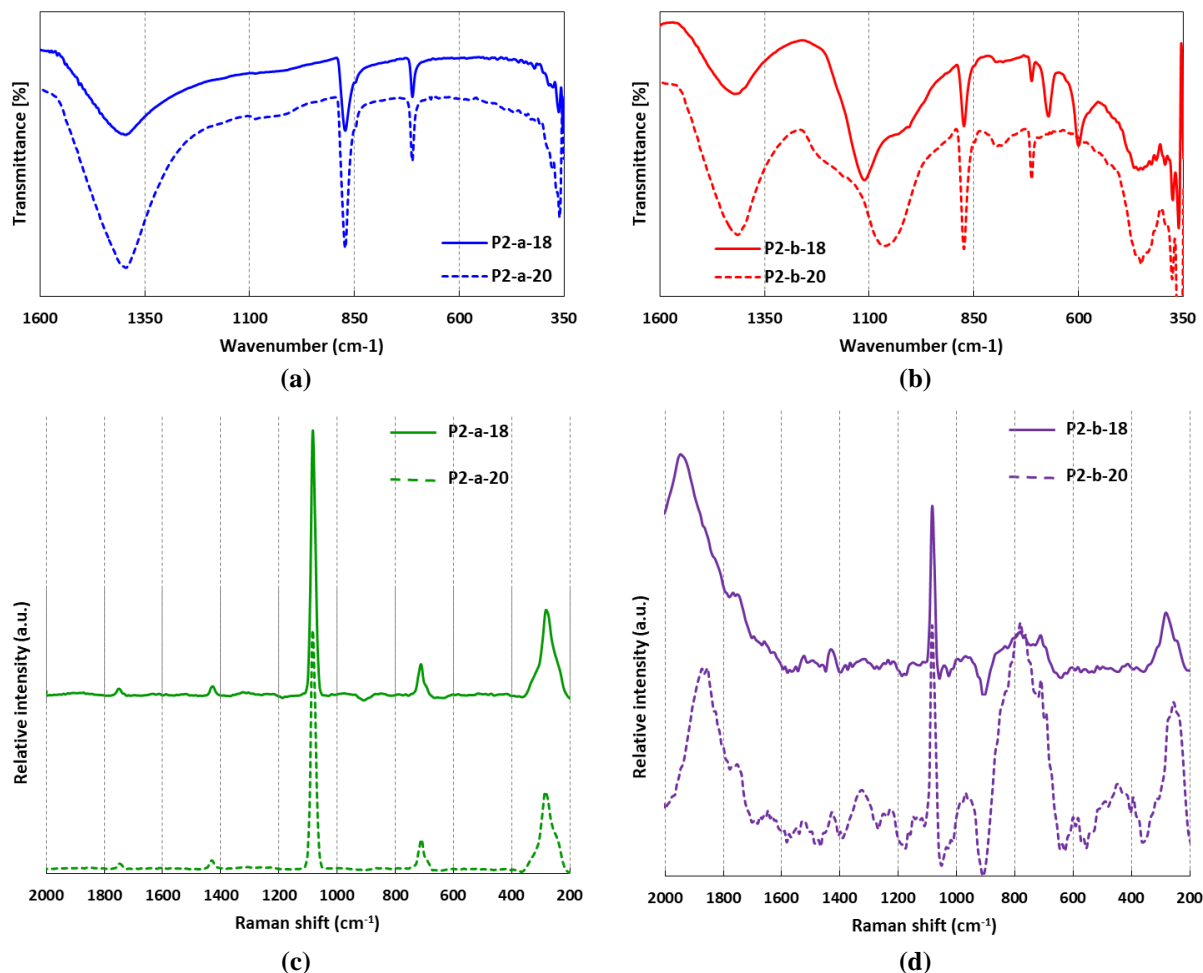


**Figure 3. Overlaps of Fourier transform infrared (FTIR) and Raman spectra for construction materials based on type and year of sampling – point P2: (a), (b) – FTIR spectra; (c), (d) – Raman spectra.**

In the Raman spectra of the samples are observed sharp and narrow Raman bands at  $1085 \text{ cm}^{-1}$  and  $284 \text{ cm}^{-1}$  corresponding to calcite [30, 34, 49]. This last peak at  $284 \text{ cm}^{-1}$  was not observed at lower relative humidity, which may be due to an increase in the calcite crystallinity at higher relative humidity. There are also portlandite signals around  $356 \text{ cm}^{-1}$ . Raman bands from  $709\text{--}712 \text{ cm}^{-1}$  could correspond to the presence of aragonite [30]. In the Raman spectra of the sample exposed to high relative humidity (90%) the observed Raman bands are located at  $1085 \text{ cm}^{-1}$ ,  $709\text{--}711 \text{ cm}^{-1}$  and around  $280 \text{ cm}^{-1}$  ( $276\text{--}284 \text{ cm}^{-1}$ ), the three of them corresponding to calcite which would mean an increase of the amount and crystallinity of this phase in the sample [30, 49]. It is therefore possible in solutions saturated with respect to vaterite that the crystallization rate of calcite becomes predominant; this could partially explain that at a higher relative humidity values there is a higher precipitation of calcite compared to the other metastable polymorphic phases. Besides calcite, quartz ( $\alpha\text{-SiO}_2$ , Raman bands at  $460 \text{ cm}^{-1}$ ) and gypsum (Raman bands at 416, 490, 617,  $1135 \text{ cm}^{-1}$ ) were found; the presence of both is common in mortars [34, 49]. As was Lopez-Arce et al. [30] have mentioned, higher values of relative humidity (75%–90%) gives rise to amorphous

calcium carbonate and monohydrocalcite, calcite, aragonite and vaterite, faster carbonation and larger particles sizes with higher crystallinity compared to lower relative humidity (33%-54%) that gives rise mainly to portlandite and vaterite, slower carbonation and smaller particle sizes with lower crystallinity.

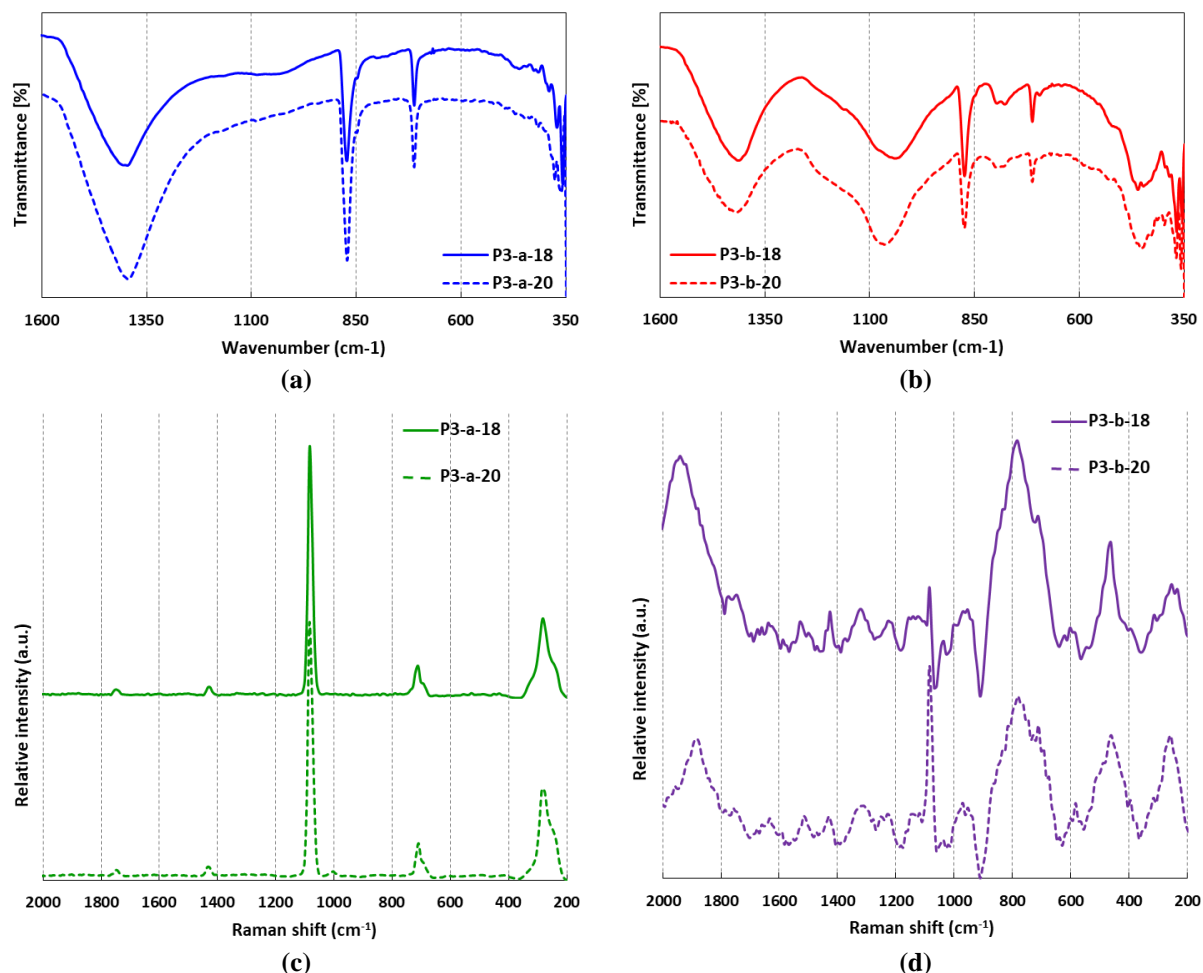


**Figure 4. Overlaps of Fourier transform infrared (FTIR) and Raman spectra for construction materials based on type and year of sampling – point P3: (a), (b) – FTIR spectra; (c), (d) – Raman spectra.**

In the stone binder FTIR spectra the presence of carbonate minerals overlaps silica / silicates ones, still being noticed weak intensity bands around  $800\text{ cm}^{-1}$  (possibly due to disordered silica) and  $470\text{ cm}^{-1}$  (deformation of tetrahedral  $\text{SiO}_4$  in silica-containing minerals) [35]. The presence of both calcite minerals and silica-containing minerals absorption bands suggests that the limestone is composed of calcite crystals and amorphous silica originating from the diatoms. The main calcium carbonate bands are present at  $712$ ,  $874$  and  $1795\text{ cm}^{-1}$ . In addition, Si-O stretching vibrations at  $1111$ ,  $1054$ ,  $1060$  and  $969\text{ cm}^{-1}$  and a weak single common band for all samples at  $795\text{ cm}^{-1}$ ; doublet originating from Si-O-Si bending vibrations that normally appears at  $798\text{-}779\text{ cm}^{-1}$  is overlapping with the in-plane bending vibrations of carbonate ion. [35, 50, 51]. The presence of amorphous silica is suggested by the presence of strong Si-O stretching band near  $1050\text{ cm}^{-1}$  that has a recognizable asymmetric shape from a shoulder near  $1200\text{ cm}^{-1}$  [41, 52]. The strong unique absorption band (for hydrated carbonates this absorption band is split) due to carbonate anion (C-O stretching vibrations) in the  $1550\text{-}1350\text{ cm}^{-1}$  region coupled with sharp band in the region of  $900\text{-}650\text{ cm}^{-1}$  (carbonate bending vibrations), confirm the presence of anhydrous compounds [47, 53];

the mentioned FTIR spectral features are present for both stone slab (intense bands around 1395, 872 and 712  $\text{cm}^{-1}$ ) and binder (intense bands around 1415, 873 and 712  $\text{cm}^{-1}$ ) samples.

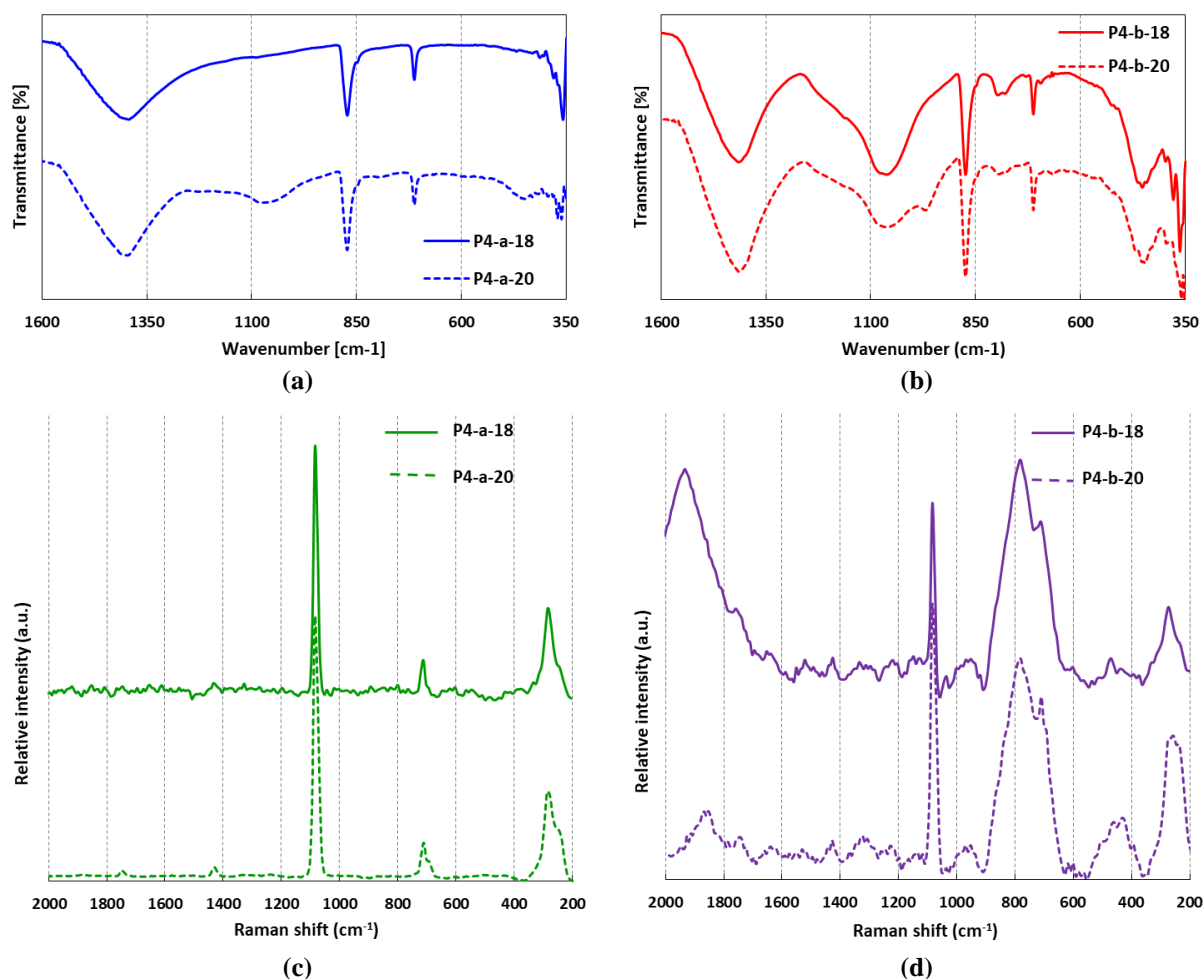


**Figure 5. Overlaps of Fourier transform infrared (FTIR) and Raman spectra for construction materials based on type and year of sampling – point P4: (a), (b) – FTIR spectra; (c), (d) – Raman spectra**

The predominant presence of calcite in the binder could be an argument for carbonation of the material, but since only the surface was analyzed, this is an expected result. The first millimeters of even new binders/mortars would carbonate in a relatively young age hence the old ones could even be completely carbonated. The normal vibrational modes of the calcite structure are derived by inversion symmetry of the crystal and hence none of the modes is simultaneously infrared and Raman active [53-55]. In the FTIR spectra of both stone and binder samples, the out-of-plane bending, the symmetric stretching and the in-plane bending modes of the carbonate ion group are found active. Besides the first order internal modes, the combination modes have also been observed. The band positions of the Raman and infrared active modes of calcite found in limestone match the values of calcite reference bands [56-59]. The minor shift in positions may be due to the effect of trace metal contents and natural impurities present in the samples. It is observed from the infrared and Raman spectra of limestone that the symmetric stretching vibration gives rise to a very strong Raman band at 1085  $\text{cm}^{-1}$ , which is normally inactive in infrared but still noticed for P1 and P2 stone samples as low intensity bands. Also as is pointed out by other studies [60-63] although fundamental absorptions or vibrations are visualized as intense bands or peaks, the infrared spectrum is complex due the presence of three types of bands: weak overtone, combination, and difference bands [61].

### 3.2. INDOOR MICROCLIMATIC MONITORING

The monument envelope is continuously exposed to the climatic conditions produced by the natural environment. It is the outside temperature and humidity (Figs. 6-8, Tables 5-6) that governs the loss and gain of heat and moisture; as other studies [63, 64] have mention, the ability of the building/envelope to shield the interior climate against the exterior influence depends on the location, the architectural design and the materials and thickness of the structure. The air tightness of the envelope also has a significant influence on the climatic stability because heat and humidity are exchanged by infiltration of air. A thorough analysis and understanding of the hygrothermal performance of the envelope is also required to select the right measures and to understand their consequences.

**Table 5. Minimum and maximum values of indoor microclimatic variables (temperature and relative humidity), recorded by mobile device.**

Microclimatic variable		Measurement point				Time interval for data acquisition
		P1	P2	P3	P4	
<b>August 2018<sup>a</sup></b>						
Temperature [°C]	MIN	22.6	22.8	22.9	23.0	Recording frequency of 40 minutes daytime (09:00 – 19:40, time slot)
	MAX	34.8	35.1	34.9	35.0	
Relative humidity [%]	MIN	78.2	76.5	76.8	78.8	
	MAX	94.2	93.4	93.6	94.0	
<b>August 2020<sup>b</sup></b>						
Temperature [°C]	MIN	20.4	20.4	28.5	29.6	Recording frequency of 40 minutes daytime (09:00 – 19:40, time slot)
	MAX	30.3	30.3	30.4	30.5	
Relative humidity [%]	MIN	83.0	80.0	80.0	81.0	
	MAX	97.0	95.0	95.0	96.0	
<sup>a</sup> Data acquisition: 5-11 August 2018; <sup>b</sup> Data acquisition: 22-26 August 2020; MIN, MAX – minimum and maximum value recorded on the monitoring period						

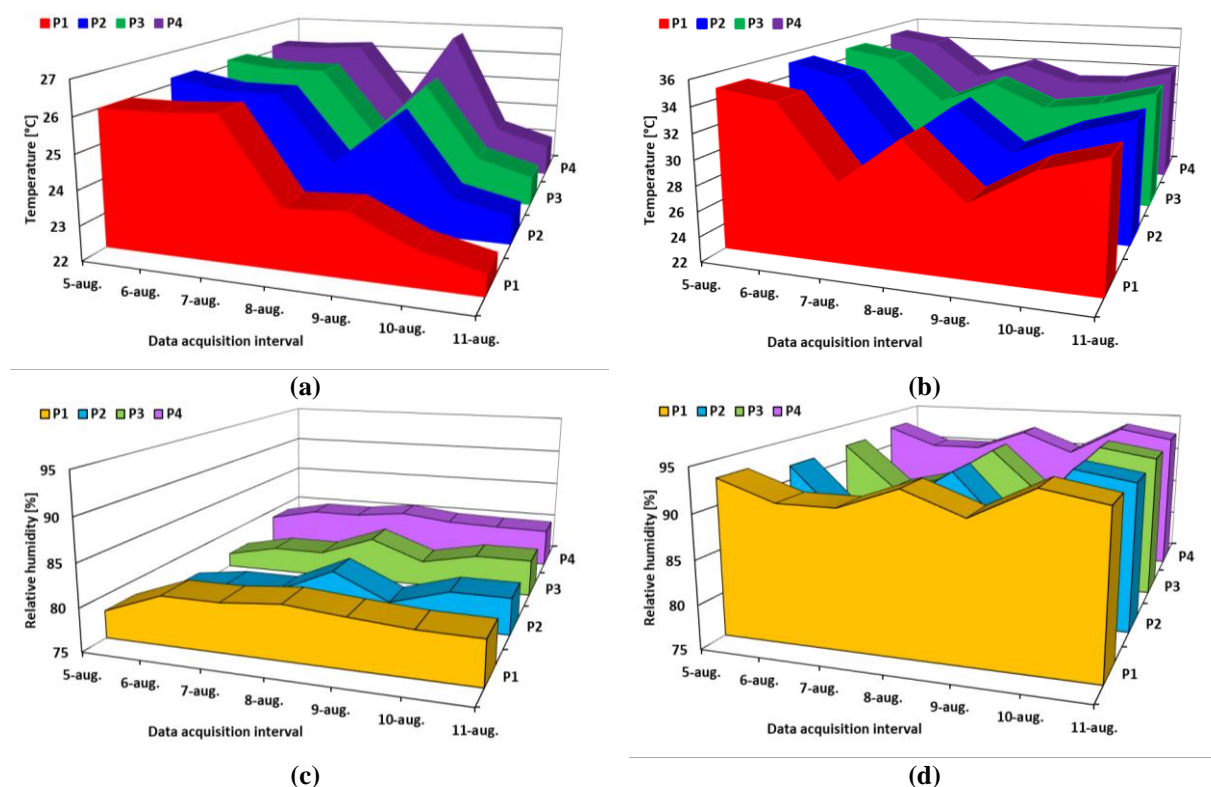


**Figure 6. Indoor microclimatic variables recorded – mobile device – for 2018 year: (a) minimum and (b) maximum temperature, (c) minimum and (d) maximum relative humidity.**

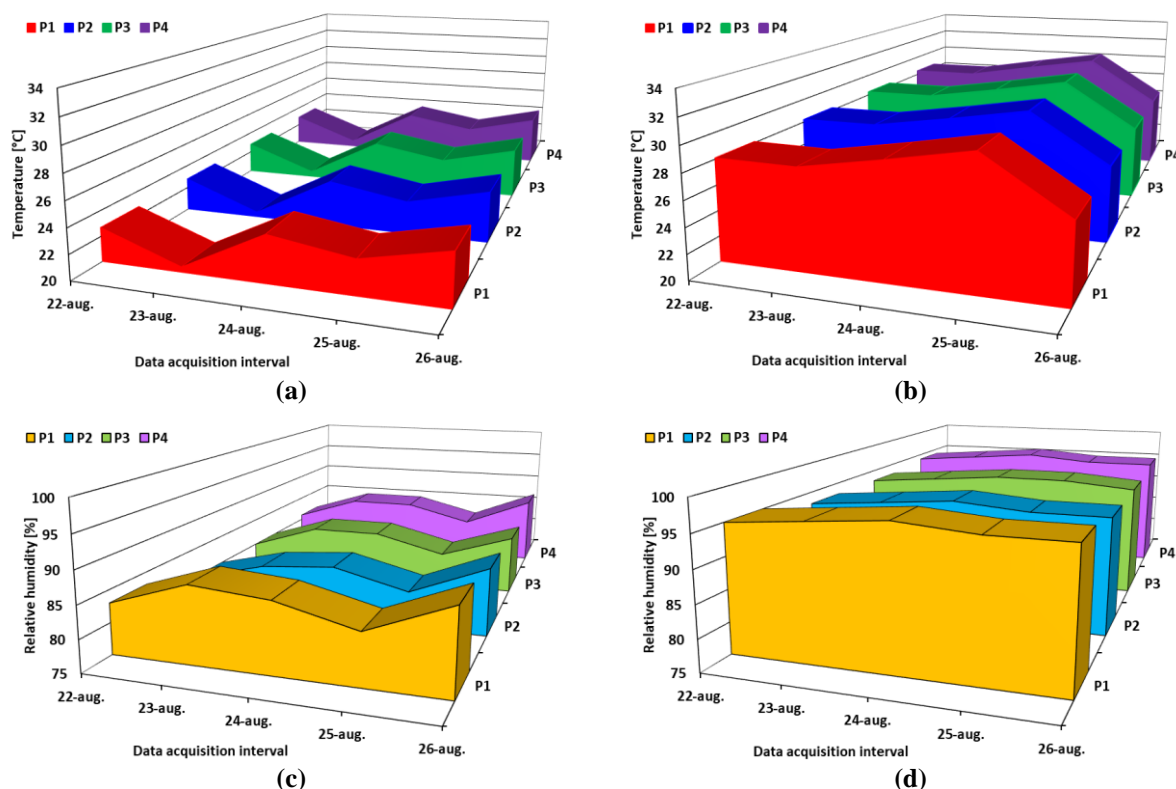


Figure 7. Indoor microclimatic variables recorded – mobile device – for 2020 year: (a) minimum and (b) maximum temperature, (c) minimum and (d) maximum relative humidity.

Table 6. Minimum and maximum values of indoor microclimatic variables (temperature and relative humidity), recorded by meteorological station.

Microclimatic variable			Time interval for data acquisition
<b>August 2018<sup>a</sup></b>			
Temperature [°C]	MIN	22.8	Recording frequency of 10 minutes continuously during monitoring period
	MAX	34.4	
Relative humidity [%]	MIN	75.0	
	MAX	94.0	
<b>August 2020<sup>b</sup></b>			
Temperature [°C]	MIN	20.5	Recording frequency of 10 minutes continuously during monitoring period
	MAX	30.7	
Relative humidity [%]	MIN	78.0	
	MAX	96.0	

<sup>a</sup>Data acquisition: 5-11 August 2018; <sup>b</sup>Data acquisition: 22-26 August 2020; MIN, MAX – minimum and maximum value recorded on the monitoring period

The values of the indoor temperature recorded with the mobile device during the monitoring period August 2018 indicate a small and constant difference at the level of the four measurement points: 3.3÷3.8°C (variation interval of the minimum temperature) and 4.1÷7.0°C (variation interval of maximum temperature). There is also a constant difference between the maximum and the minimum value (12.0÷12.3°C) at the level of each point during the monitoring (Fig. 9). The values recorded with the weather station are approximately in the same intervals, 3.4°C (for the minimum value) and 3.5 (for the maximum value) respectively with a difference of 11.5°C (between the maximum and the minimum value) at the level of point P4.

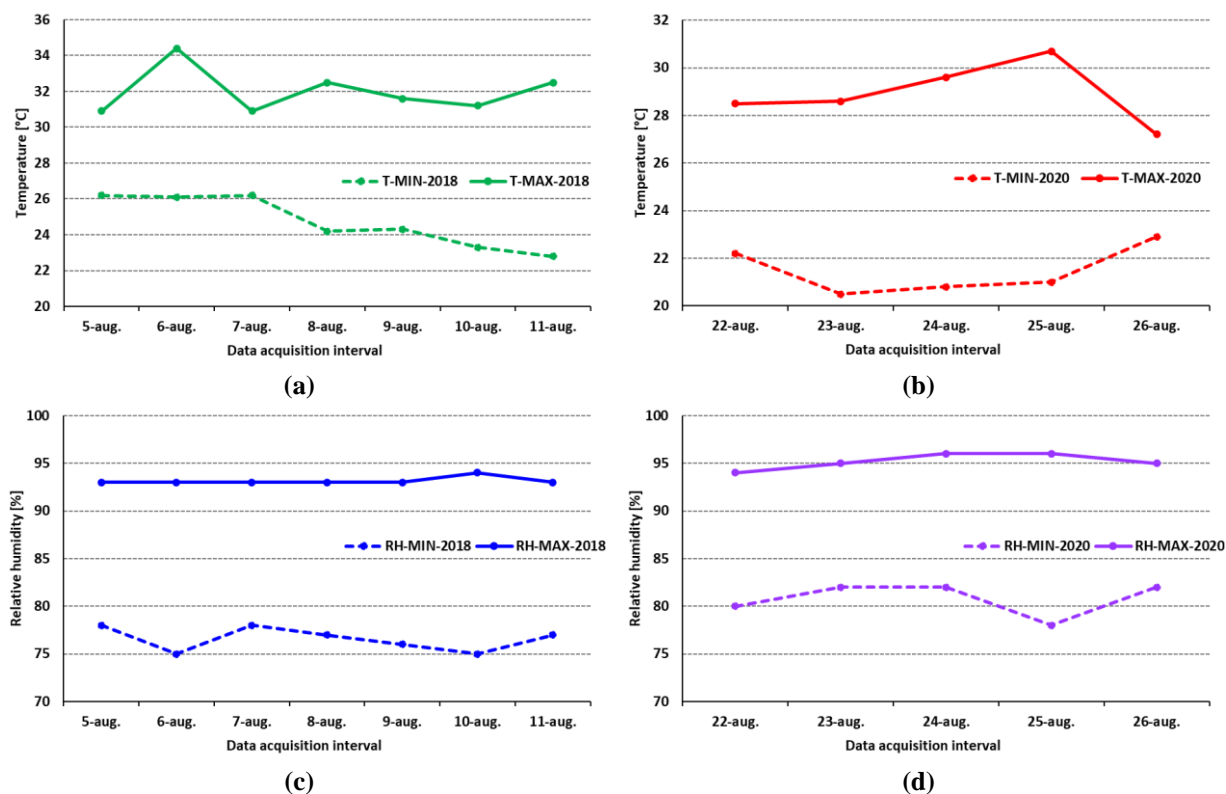


Figure 8. Indoor microclimatic variables recorded with meteorological station: (a), (b) – minimum and maximum temperature; (c), (d) – minimum and maximum relative humidity.

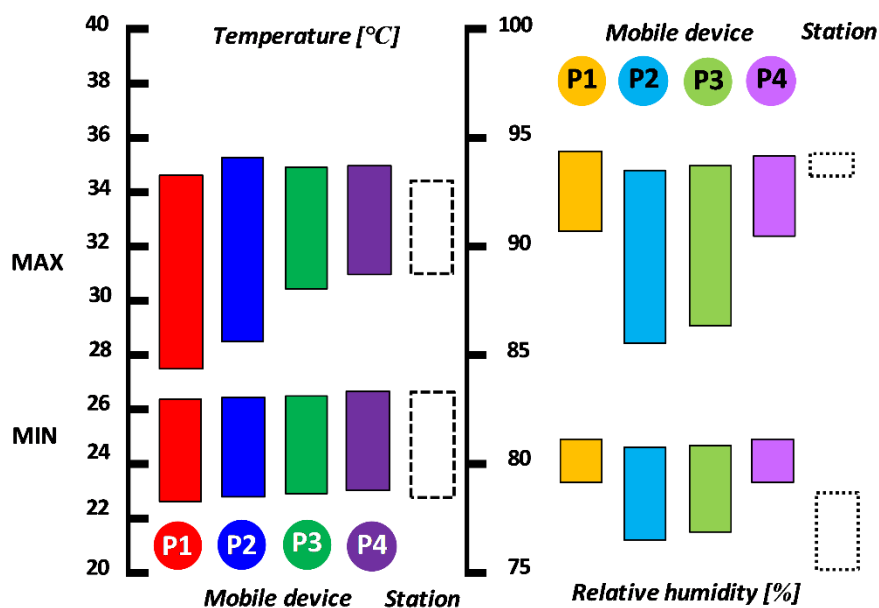
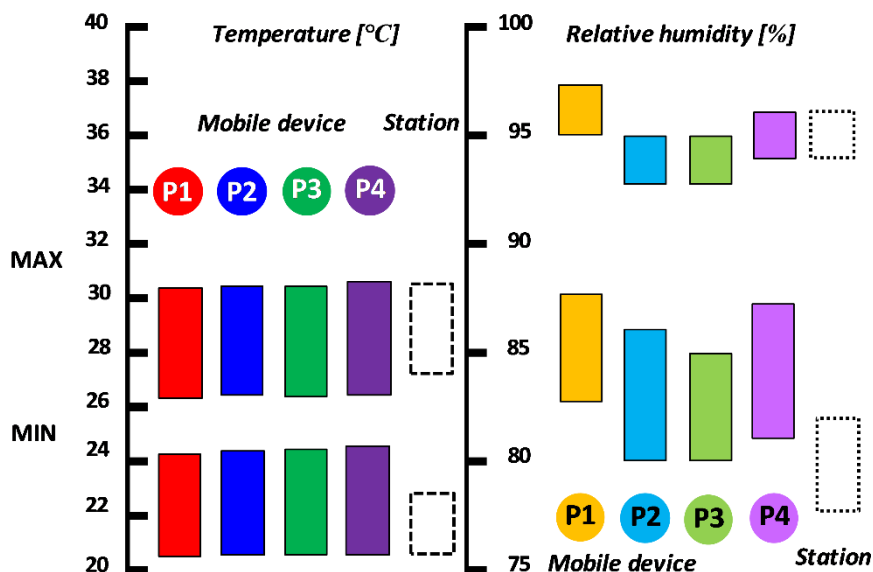


Figure 9. Variation range for maximum and minimum indoor microclimatic variables recorded during August 2018 monitoring period.

During the monitoring period August 2020, the variation intervals recorded with the mobile device the indoor temperature at the level of the four measurement points were:  $3.7\div 3.8^{\circ}\text{C}$  (variation interval of the minimum temperature) and  $4.0\div 4.1^{\circ}\text{C}$  (variation interval of maximum temperature). There is also a constant difference ( $9.9^{\circ}\text{C}$ ) between the maximum and minimum value at each point during monitoring (Fig. 10). The values recorded with the weather station are approximately in the same intervals,  $2.4^{\circ}\text{C}$  (for the minimum value) and

3.5°C (for the maximum value) respectively with a difference of 10.2°C (between the maximum and the minimum value) at the level of point P4.



**Figure 10.** Variation range for maximum and minimum indoor microclimatic variables recorded during August 2020 monitoring period

The relative humidity (RH) registered increased values (76.5÷94.2%) during the monitoring period August 2018, variation intervals registered with the mobile device being between 2.2÷4.0% (minimum RH) and respectively 3.5÷8.0% (maximum RH); the observed difference (15.2-16.9%) between the maximum and the minimum of the values recorded during the monitoring at the level of the four measurement / sampling points is also notable. Variation intervals in the case of measurements made with the weather station were between 75÷78% (minimum RH) and 93÷94% (maximum RH), respectively.

During the monitoring carried out in August 2020 with the mobile device, RH also recorded increased values (80-97%), the variation intervals recorded at the level of measurement / sampling points being between 5÷6% (minimum RH) and respectively 2% (maximum RH) with a difference of 14÷15% between the maximum and minimum of the registered values. Variation intervals in the case of measurements made with the weather station were between 78÷82% (minimum RH) and 94-96% (maximum RH).

As regards the air RH, in both summer periods the highest values have been found in the lower and the highest part of the structure (points P1 and P4, respectively). The lowest values have been recorded in the same middle zone (points P2 and P3), changing in function of the hour. In the case of the values of the maximum temperature registered in both monitoring periods, a slightly increasing tendency is observed, the highest value being the one corresponding to points P4 and P3. It is important in the circumstances of the monument to consider that monitoring had established that the building had relative little thermal buffering. Ventilation is often challenging in the context of historic structures: sealing a historic edifice is both practically impossible and can actually accelerate damage through raising indoor RH; at the other extreme, draughts created by open doors and windows can be equally deleterious, as they provide for almost uncontrolled air exchange.

Building materials of cultural/historical monuments such as natural stones like limestone, investigated in the present study, can undergo, over time, degradation of their mechanical and petrophysical properties, particularly due to mechanical stress and long-term environmental conditions. Other studies [65-67] on similar building material have pointed out that micro-cracks may appear within the stone microstructure leading, under environmental

cycles, to macro scale decay as scaling or fragmentation. Low-high temperature cycles together with high constant RH levels can lead to such environmental stresses on stone exposed surfaces even in case of those protected/enveloped like Tropaeum Traiani monument, Adamclisi. Limestone degradation is accelerated under high humidity conditions.

It seems to be reasonable to assume a high moisture load of the structure, where especially unfavorable indoor air humidity conditions must be supposed. Unfortunately, there are hardly any measured data available for such cases so that it is difficult to decide, whether the respective specifications of the WTA guideline 6-2 (International Association for Science and Technology of Building Maintenance and Monument Preservation) or CSN EN 15026 (Hygrothermal performance of building components and building elements-Assessment of moisture transfer by numerical simulation) are better suited.

#### 4. CONCLUSIONS

The surface of original structure/construction materials used until present seems not to be affected at major scale by the indoor microclimate variables. But even high relative humidity levels recorded promote/gives rise to amorphous calcium carbonate, calcite, aragonite and vaterite highlighted by vibrational spectroscopy data (FTIR and Raman), as a first effect, the development of biological organism is enhanced, depending on the characteristics of the substrate. Second, atmospheric pollutants can be dissolved easier in the humidity existing in the porous material, and lastly, if the waterflow inside the stone is not homogeneous, cracks could appear due to differences in permeability.

For decades and even more, the indoor climate was not controlled with respect to conservation. Any object/material holds a memory of previous climate which may have altered its appearance or reduced its lifetime. No matter how perfectly the future indoor climate is controlled today, it will not heal the damages of failures in the past. Even a minor adjustment in climate control will increase the expected lifetime of most cultural and historical assets or reduce the need for conservation and maintenance. Often, indoor climate control is a very cost-efficient tool for preventive conservation and furthermore, a better understanding of the climate requirements will allow for an optimal use of energy.

With respect to the conservation of the original materials, the knowledge of traditional binder technologies and stone-based materials coupled with the monitoring of local environmental variables are very important to interpret their origin, time evolution and perspectives. Nevertheless, investigations of characteristics of traditional mortars/binders could clarify both preparation technologies of the mixtures and application procedures. Degradation in the general state of conservation is made worse by interaction with environmental agents and by interaction with atmospheric pollution and increases with time. Any plan for conservation treatment on historic and cultural heritage assets must consider the historical, stylistic-aesthetic, scientific, and technical aspects.

**Acknowledgement:** *This research was funded by the project 51PCCDI/2018, financed by Romanian National Authority for Scientific Research (UEFISCDI) "New diagnosis and treatment technologies for the preservation and revitalization of archaeological components of the national cultural heritage" and by bilateral Project 04-4-1121-2015/2020, between Valahia University of Targoviste and Joint Institute for Nuclear Research, Dubna, Moscow Region; Protocol 4755-4-2018/2020 "Micro-structural and compositional characterization*

of supports and coating layers on different substrates applied in biomaterials, photoelectrochemicals catalysis and cultural heritage”.

## REFERENCES

- [1] Tiano, P., *Proceedings ARIADNE Workshop 9 – historic materials and their diagnostic*, 1-37, 2002.
- [2] Radulescu C., Stihl C., Ion R.M., Dulama I.D., Stanescu S.G., Stirbescu R.M., Teodorescu S., Gurgu I.V., Let D.D., Olteanu L., Stirbescu N.M., Bucurica I.A., Olteanu R.L., Nicolescu C.M, *Atmosphere*, **10**(10), 595, 2019.
- [3] Jedrzejewska, H., *The Conservation of Stone II*, Part A, R. Rossi-Manaresi Ed., Bologna, 195-204, 1981.
- [4] Bologna, A.S., Gramescu, A.M., *Tropaeum Augusti (France) and Tropaeum Traiani (Romania): A Comparative Study*, 1-20, in *Heritage*, Editor Turcanu\_Carutiu D., IntechOpen, 2020.
- [5] Russell, B.J., *Gazetteer of Stone Quarries in the Roman World*, V. 1.0, 2013. Available online; last accessed 19.11.2020.  
[www.romaneconomy.ox.ac.uk/database/stone\\_quarries\\_database/](http://www.romaneconomy.ox.ac.uk/database/stone_quarries_database/).
- [6] Florescu, F.B., *Monumentul de la Adamklissi*, second edition, Ed. Acad. Rom., 1961.
- [7] Radulescu, A., *Pontica*, **5**, 177, 1972.
- [8] Radulescu, A., *Pontica*, **10**, 9, 1978.
- [9] Radulescu, A., *Tropaeum Traiani – Monument si cetate*, Ed. Sport Turism, Bucuresti, 1988.
- [10] Sampetru, M., *Tropaeum Traiani – Monumente romane*, Ed. Acad. Rom., Bucuresti, 1984.
- [11] Sramek, J., *Alteration et protection des monuments en pierre: Colloque international / Deterioration and Protection of Stone Monuments*, International Symposium, June 5-9, Paris, 1978.
- [12] Faraone, G., *Restauro e citta*, **7**, 56, 1987.
- [13] Rao, G.B., *Journal of Archaeological Chemistry*, **2**, 39, 1984.
- [14] Ion R.-M., Iancu L., Vasilievici G., Grigore M.E., Andrei R.E., Radu G.-I., Grigorescu R.M., Teodorescu S., Bucurica I.A., Ion M.-L., Gheboianu A.I., Radulescu C., Dulama I.D., *Coatings*, **9**, 231, 2019.
- [15] Ion R.M., Bakirov B.A., Kichanov S.E., Kozlenko D.P., Belushkin A.V., Radulescu C., Dulama, I.D. Bucurica, I.A., Gheboianu A.I., Teodorescu, S., Stirbescu, R.M., Ianu L., David M.E., Grigorescu R.M., *Applied Sciences*, **10**(11), 3781, 2020.
- [16] Bradley, S., *Conservation News*, **34**, 24, 1987.
- [17] Abd El-Hady, M.M., *6<sup>th</sup> International Congress on Deterioration and Conservation of Stone*, **1**, comp., Ciabach J., Torun, Poland, Nicholas Copernicus University Press Department, 387-394, 1988.
- [18] Domasłowski, W., Kesy-Lewandowska, M., *2<sup>a</sup> conferenza internazionale sulle prove non distruttive metodi microanalitici e indagini ambientali per lo studio e la conservazione delle opere d'arte*, **1**, Perugia, Italy, 17-20 April, 1-31, 1988.
- [19] Blanco, M.T., Puertas, F., Palomo, A., Accion, F., *Science, Technology, and European Cultural Heritage: Proceedings of the European Symposium*, Bologna, Italy, 13-16 June, ed. N.S. Baer, C. Sabbioni and A. Sors, Oxford and Boston: Butterworth-Heinemann, 601-606, 1991.
- [20] Gorgoni, C., Lazzarini, L., Salvadori, O., *Proceedings of the 7th International Congress on Deterioration and Conservation of Stone*, Lisbon, Portugal, 15-18 June, ed. J.D.

- Rodrigues, F. Henriques, and F.T. Jeremias, Lisbon: Laboratorio Nacional de Engenharia Civil, 531-539, 1992.
- [21] Biscontin, G., Volpin, S., *Oxalate films: Origin and meaning in the conservation of works of art*, Milan: Centro del C.N.R. "Gino Bozza", 151-163, 1989.
- [22] White, R.L., Ai, J., *Applied Spectroscopy*, **46**(1), 93, 1992.
- [23] Matteini, M., Moles, A., Giovannoni, S., *The conservation of monuments in the Mediterranean basin: Proceedings of the 3<sup>rd</sup> international symposium*, ed. V. Fassina, H. Ott, and F. Zezza, Venice, Italy, 155-162, 1994.
- [24] Zhao, C., Zhang, Y., Wang, C-C., Hou, M., Li, A., *Heritage Science*, **7**:36, 1-50, 2019.
- [25] Bintintan A., Gligor M., Radulescu C., Dulama I.D., Olteanu R.L., Stirbescu R.M., Teodorescu S., Bucurica I.A., *Analytical Letters*, **52**(15), 2348, 2019.
- [26] Bintintan A., Gligor M., Dulama I.D., Radulescu C., Stihl C., Ion R.M., Teodorescu S., Stirbescu R.M., Bucurica I.A., Pehoiu G., *Romanian Journal of Physics*, **64**(5-6), 903, 2019.
- [27] Domenech Carbo, M.T., Periz Martinez, V., Gimeno Adelantado, J.V., Bosch Reig, F., Moya Moreno, M.C.M., *Journal of Molecular Structure*, **410-411**, 559, 1997.
- [28] Silva, D.A., Wenk, H.R., Monteiro, P.J.M., *Thermochim. Acta.*, **438**, 35, 2005.
- [29] Weber, J., Gadermayr, N., Kozłowski, R., Mucha, D., Hughes, D., Jaglin, D., Schwarz, W., *Mater Charact.*, **58**, 1217, 2007.
- [30] Lopez-Arce, P., Gomez-Villalba, L.S., Martinez-Ramirez, S., Alvarez de Buergo, M., Fort, R., *Powder Technology*, **205**(1-3), 263, 2011.
- [31] Martinez-Ramirez, S., Sanchez-Cortes, S., Garcia-Ramos, J.V., Domingo, C., Fortes, C., Blanco-Varela, M.T., *Cem. Concr. Res.*, **33**, 2063, 2003.
- [32] Dandeu, A., Humbert, B., Carteret, C., Muhr, H., Plasari, E., Bossoutrot, J.M., *Chem. Eng. Technol.*, **29**(2), 221, 2006.
- [33] Kontoyannis, C.G., Vagenas, N.V., *Analyst*, **125**, 251, 2000.
- [34] Mendonca Filho, F.F., Morillas, H., Derluyn, H., Maguregui, M., Gregoire, D., *Microchemical Journal*, **147**, 905, 2019.
- [35] Boke, H., Cizer, O., Ipekoglu, B., Ugurlu, E., Serifaki, K., Toprak, G., *Construction and Building Materials*, **22**, 866, 2008.
- [36] Watt, D., *Building Pathology: Principles and Practice*, Second Edition, Blackwell Publishing, Oxford, UK, 2009.
- [37] Moropoulou, A., Bakolas, A., Bisbikou, K., *J. Cult. Herit.*, **1**, 45, 2001.
- [38] Gibbons, P., *Pozzolans for lime mortars*, Cathedral Communications Ltd., The Building Conservation Directory, Tisbury, 1997.
- [39] Chirita, C., *Cross section from Adamclisi Reconstructed Roman Monument*, 2008, based on information from <http://cimec.ro/Arheologie/tropaeum/introen/body.html>, CT-I-m-A-02567.05.
- [40] Adler, H.H., Kerr, P.F., *The American Mineralogist*, **48**, 124, 1963.
- [41] Smith, B.C., *Infrared Spectral Interpretation: A Systematic Approach*, CRC Press, Boca Raton London, New York, Washington D.C., 1999.
- [42] Zuena, M., Tomasin, P., Costa, D., Delgado-Rodriguez, J., Zenchi, E., *Coatings*, **8**, 103, 1, 2018.
- [43] Clarkson, R., Price, T.J., Adams, C.J., *J. Chem. Soc., Faraday Trans.*, **88**, 243, 1992.
- [44] Tlili, M.M., Ben Amor, M., Gabrielli, C., Joiret, S., Maurin, G., Rousseau, P., *J. Raman Spectrosc.*, **33**, 10, 2001.
- [45] Awarwal, P., Berglund, K.A., *Cryst. Growth Des.*, **3**(6), 941, 2003.
- [46] Jordan, M.M., Jorda, J., Pardo, F., Montero, M.A., *Materials*, **12**, 55, 1, 2019.
- [47] Anderson, F.A., Brecevic, L., *Acta Chem. Scan.*, **45**, 1018, 1991.

- [48] Hopkinson, L., Rutt, K., Kristova, P., Blows, J., Firth, C., *Journal of Cultural Heritage*, **16**, 822, 2015.
- [49] Saheb, M., Chabas, A., Mertz, J-D., Colas, E., Rozenbaum, O., Sizun, J-P., Nowak, S., Gentaz, L., Verney-Carron, A., *Corrosion Science*, Elsevier, **111**, 742, 2016.
- [50] Bakolas, A., Biscontin, G., Moropoulou, A., Zendri, E., *Thermochim. Acta*, 269/270, 809, 1995.
- [51] Simionescu, B., Olaru, M., Aflori, M., Doroftei, F., *European Journal of Science and Technology*, **7**(3), 85, 2011.
- [52] Derrick, M.R., Stulik, D., Landry, J.M., *Infrared Spectroscopy in Conservation Science*, Chapter 5, Spectral Interpretation, Getty Publication Virtual Library, The Getty Conservation Institute, Los Angeles, USA, 1999.
- [53] Rutt, H.N., Nicola, J.H., *J. Phys. C: Solid State Phys.*, **7**, 4522, 1974.
- [54] Gaffey, S.J., *Am. Mineral.*, **71**, 151, 1986.
- [55] Gunasekaran, S., Anbalagan, G., Pandi, S., *Journal of Raman Spectroscopy*, **37**, 892, 2006.
- [56] Legodi, M.A., DeWaal, D., Potgieter, J.H., *Appl. Spectrosc.*, **55**, 361, 2001.
- [57] Nicola, J.H., Scott, J.F., Couto, R.M., Correa M.M., *Phys. Rev. B* **14**, 4676, 1976.
- [58] Elderfield, H., *Am. Mineral.*, **56**, 1600, 1971.
- [59] Griffith, W.P., *Nature*, **224**: 264, 1969.
- [60] dos Santos, G.F., Ferrao, M.F., Wolf, C.R., *Spectrochim. Acta A Mol. Biomol. Spectrosc.*, **153**, 94, 2016.
- [61] Bauer, R., Nieuwoudt, H., Bauer, F.F., Kossmann, J., Koch, K.R., Esbensen, K.H., *Analytical Chemistry*, **80**(5), 1371, 2008.
- [62] Karoui, R., Downey, G., Blecker, C., *Chem. Rev.*, **110**(10), 6144, 2010.
- [63] Brostrom, T., Larsen, P.K., *Climate Control in Historic Buildings*, Uppsala University, National Museum of Denmark, ed. S. Carlsten, 1-73, 2015.
- [64] Okba, E.M., *International Conference "Passive and Low Energy Cooling for the Built Environment"*, Santorini, Greece, 467-473, 2005.
- [65] Stambolov, T., van Asperen de Boer, J.R.J., *The Deterioration and Conservation of Porous Building Materials in Monuments – A Review of literature*, International Centre for the Study Of The Preservation and the Restoration of Cultural Property, Second enlarged edition, Rome, Italy, 1976.
- [66] Walbert, C., Eslami, J., Beaucour, A-L., Ann Bourges, Noumowe, A., *Environ Earth Sci*, **74**(7), 1, 2015.
- [67] Corvo, F., Reyes, J., Valdes, C., Villasenor, F., Cuesta, O., Aguilar, D., Quintana, P., *Water Air Soil Pollution*, **205**, 359, 2010.